Pergamon

Int. J. Multiphase Flow Vol. 24, No. 4, pp. 605–615, 1998

Printed in Great Britain
PII: S0301-9322(97)00083-9
0301-9322/98 $19.00 + 0.00

THEORETICAL AND EXPERIMENTAL INVESTIGATIONS ON INSTABILITY OF AN ELECTRICALLY CHARGED LIQUID JET

P. H. SON[1] and K. OHBA[1]

[1]Department of Mechanical and Systems Engineering, Kansai University, 3-3-35, Yamate-cho, Suita, Osaka 564, Japan

(Received 24 January 1997; in revised form 23 October 1997)

Abstract—By employing Lagrange equation of motion, a dispersion equation that accounts for the growth of axisymmetric, as well as non-axisymmetric waves on an electrically charged liquid jet is derived in this work, with considering the electric field configuration of a needle-plate apparatus for liquid spraying. The available theory is capable of predicting the phenomenon of both of axisymmetric and non-axisymmetric deformations of the liquid jet, which has long been observed in practice. It is demonstrated that there exist certain ranges of such parameters as applied voltage and needle-plate distance where the axisymmetric and non-axisymmetric modes of instability take place. The axisymmetric mode has a dominant effect at low electric field strength. As the electric field strength is increased, the non-axisymmetric mode is intensified. The present theory indicates that the critical wavelength, and thus, the droplet size are decreased with increasing applied voltage and/or shortening needle-plate distance, which is consistent with the experimental results. © 1998 Elsevier Science Ltd. All rights reserved

Key Words: electrostatic spraying, charged liquid jet, instability, dispersion equation, growth rate, breakup wavelength, axisymmetric mode, non-axisymmetric mode

1. INTRODUCTION

An electrostatic liquid spraying process has many practical applications, such as the sources for spacecraft propulsion, ink-jet printer, paint spraying, crop spraying, fuel spraying in combustion systems, etc. Many aspects related to the theory and practice of electrostatic spraying are reviewed due to Bailey (1974, 1986). The most common electrostatic liquid spraying apparatus consists of an electrically grounded plate and a capillary tube which is raised to a high electric potential. The liquid is passed through the capillary tube and subjected to an intense electric field. As a result, a thin jet is emanated from the tip of capillary tube and breaks up into fine droplets. The process of disintegration of an electrically charged liquid jet is one that involves an instability at a liquid interface owing to electrostatic force, produced by induced charges, overcoming the surface tension force of the liquid.

Some theoretical studies have been carried out in order to investigate the mechanism of the breakup of an electrically charged liquid jet. According to Schneider *et al.* (1967), the surface of liquid jet is assumed to be subjected to an initial small axisymmetric disturbance. This disturbance will grow, giving the liquid jet a varicose form and eventually causing the breakup of the jet. However, many experimental and practical studies clearly show that with the increasing of the applied electric potential, non-axisymmetric disturbances are amplified and the form of liquid jet becomes sinuous, see Cloupeau and Prunet-Foch (1990, 1994). Huebner and Chu (1971) considered both the axisymmetric and non-axisymmetric modes of liquid jet instability, but for the case of needle-cylinder electrodes configuration. Since the electric potential for needle-plate electrodes configuration is different compared to the needle-cylinder configuration, the theoretical analysis for this case is necessary.

In this work, we conduct the instability analysis of the electrically charged liquid jet for the case of needle-plate apparatus for liquid spraying. The dispersion equation for the charged liquid jet is derived, based on Rayleigh's technique, i.e. the Lagrange equation of motion for the generalized coordinate, see Lord Rayleigh (1882, 1945). The electric field configuration of the

needle-plate apparatus is considered when defining the electrostatic potential energy. Then the axisymmetric and non-axisymmetric modes of the liquid jet instability are investigated based on the derived dispersion equation. On the other hand, the experiments are conducted using a needle-plate apparatus for liquid spraying. The behavior of the liquid jet and its disintegration process are visualized. Furthermore, the experimental results are compared with the calculated ones obtained from the theoretical analysis.

We build our work as follows. The derivation of the dispersion equation is given in Section 2. Detailed results of the calculation of the growth rate of disturbations and critical wavelengths are presented and discussed in Section 3. Then the theoretical and experimental results are compared and discussed in Section 4. Finally, some concluding remarks are given in Section 5.

2. MATHEMATICAL FORMULATION AND SOLUTION

We consider an infinitely long cylindrical jet of radius a of an incompressible and inviscid liquid with uniform density ρ. The liquid jet is assumed to be injected with low velocity into the stationary air. We assume that gravity is negligible on the lengthscales of interest.

The surface of the perturbed jet (see figure 1) is represented in cylindrical coordinates (r, θ, z) by the equation

$$r_0 = a_0 + c \cos m\theta \cos kz \qquad [1]$$

where a_0 is a mean radius, c is an infinitesimal deviation from the cylindrical shape of the liquid jet ($c \ll a_0$ and proportional to $e^{\omega t}$, ω is the complex frequency and named as the growth rate of the disturbance, t is time), m and k are the azimuthal and axial wave-numbers, respectively. Here $k = 2\pi/\lambda$ is real and positive, λ is wavelength and m is integral.

The analysis is carried out for the axisymmetric instability mode $m = 0$, as well as the non-axisymmetric instability modes $m \neq 0$. For the mode with $m = 0$ [see figure 1(a)], the cross section of the jet is circular and its radius varies only along the axial direction z. This mode is often called the varicose mode. For the mode with $m = 1$ [see figure 1(b)], the cross section of the jet is still nearly circular with constant size in the axial direction. The axis of the jet, however, is sinuous. This mode is commonly referred to as the sinuous or "kink" mode.

Here a_0 is related to the original undisturbed jet radius a by the requirement that the volume of liquid per wavelength remains unchanged. This means

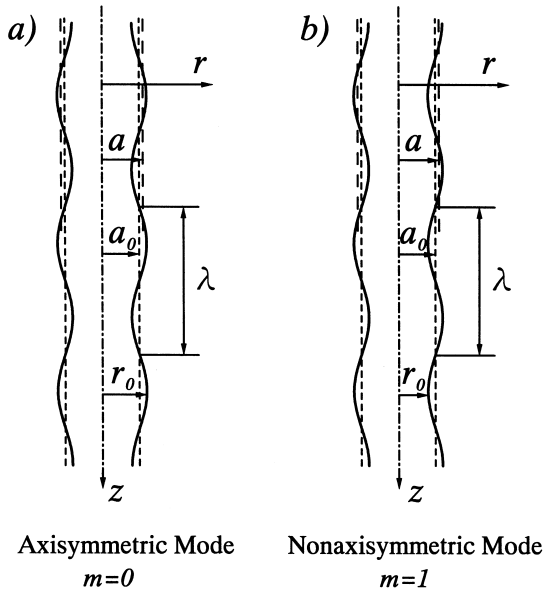

Figure 1. Instability modes of liquid jet deformation.

$$\int_0^{\lambda}\int_0^{2\pi}\frac{1}{2}r_0^2\,\mathrm{d}\theta\,\mathrm{d}z=\pi a^2\lambda \qquad [2]$$

which gives

$$a^2=a_0^2+\frac{1}{4}(1+\delta_m)c^2 \qquad [3]$$

where

$$\delta_m=1 \text{ as } m=0$$
$$\delta_m=0 \text{ as } m\geq 1$$

Following Rayleigh, we will carry out the analysis based on the Lagrange equation of motion for the generalized coordinate c.

The potential at any point in the vicinity of the jet V is found as the sum of two potentials: one due to a charged circular cylinder of liquid, V_c, and the other appropriate harmonic term due to the electrical charge to account for the surface perturbation, V_p, i.e.

$$V=V_c+V_p \qquad [4]$$

For the case of needle-plate configuration (see figure 2) the electric field strength and potential were calculated by Jones and Thong (1971), using the method of images. The potential is given by these authors as

$$\phi=\frac{-\sigma_s}{4\pi\varepsilon_0}\ln\left[\frac{\sqrt{r^2+(h-z)^2}+(h-z)}{\sqrt{r^2+(h+z)^2}+(h+z)}\right] \qquad [5]$$

where σ_s is surface charge density per unit length, ε_0 is permittivity of the medium surrounding the liquid jet and h is needle-plate distance.

At the tip of the needle, i.e. $r=r_c$, $z=h$, we have $\phi=V_0$. Here r_c is needle radius, V_0 is applied voltage. Besides, in the vicinity of the tip we can accept $h\gg r$ and $z\approx h$. Then [5]

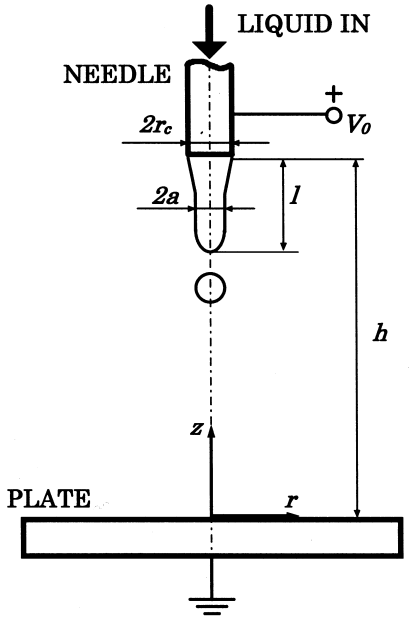

Figure 2. Needle-plate scheme for electrostatic spraying of liquid.

becomes

$$\phi = \frac{V_0}{\ln 4h/r_c} \ln 4h/r$$

By making use of this result and assuming that the potential on the surface of the unperturbed jet is constant and equal to applied voltage, we can express the potential in the vicinity of the unperturbed jet at a distance r from the jet axis approximately as

$$V_c = \frac{V_0}{\ln 4h/a} \ln 4h/r \quad [6]$$

The surface is perturbed according to [1], giving rise to field perturbations proportional to $\cos m\theta \cos kz$, so that the potential of the perturbed jet V_p takes the form

$$V_p = C_1 R_{(r)} \cos m\theta \cos kz \quad [7]$$

where $R_{(r)}$ is certain function of the coordinate r and C_1 is constant.

V_p satisfies the Laplace equation

$$\nabla^2 V_p = 0 \quad [8]$$

Writing this equation in cylindrical coordinates we obtain the Bessel equation

$$\frac{\partial^2 R}{\partial r^2} + \frac{1}{r}\frac{\partial R}{\partial r} - \left(k^2 + \frac{m^2}{r^2}\right) R = 0 \quad [9]$$

which gives the solution

$$R_{(r)} = C_2 I_m(kr) + C_3 K_m(kr) \quad [10]$$

Here, $I_m(kr)$ and $K_m(kr)$ are the modified Bessel functions of the first kind and the second kind, respectively, both of integral order m, C_2 and C_3 are constants. Therefore

$$V_p = [C_4 I_m(kr) + C_5 K_m(kr)] \cos m\theta \cos kz \quad [11]$$

The function $I_m(kr)$ is infinite at $kr = \infty$. This makes it unsuitable for the region outside the jet and must be excluded, i.e. $C_4 = 0$. As a result, the potential V_p gets the following form

$$V_p = C_5 K_m(kr) \cos m\theta \cos kz \quad [12]$$

Substitution of [6] and [12] into [4] gives

$$V = \frac{V_0}{\ln 4h/a} \ln 4h/r + C_5 K_m(kr) \cos m\theta \cos kz \quad [13]$$

It is assumed that the potential on the surface of the jet is constant at V_0, i.e. $V = V_0$ at $r = r_0$. With the use of this boundary condition and let $a_0 = a$, $K_m(kr_0) \approx K_m(ka)$, we obtain

$$C_5 = \frac{cV_0}{a \ln 4h/a} \frac{1}{K_m(ka)} \quad [14]$$

Therefore, the electric potential in the vicinity of the liquid jet becomes

$$V = \frac{V_0}{\ln 4h/a} \left[\ln 4h/r + \frac{c}{a} \frac{K_m(kr)}{K_m(ka)} \cos m\theta \cos kz \right] \quad [15]$$

The surface charge density is calculated according to

$$\sigma_s = -\varepsilon_0 (\mathbf{n} \text{grad} V)_{r=r_0} = -\varepsilon_0 \left. \frac{\partial V}{\partial n} \right|_{r=r_0} \quad [16]$$

where $\mathbf{n}$ is unit vector perpendicular to the surface.

Since σ_s is assumed to vary only in the radial direction, we have

$$\sigma_s = -\varepsilon_0 \left.\frac{\partial V}{\partial r}\right|_{r=r_0} = -\frac{\varepsilon_0 V_0}{\ln 4h/a}\left[-a^{-1} + \frac{c}{a^2}\cos m\theta \cos kz + \frac{ck}{a}\frac{K'_m(ka)}{K_m(ka)}\cos m\theta \cos kz\right] \quad [17]$$

with neglecting the higher order in c. Here we take the approximation

$$K'_m(ka) \approx K'_m(kr_0) = \left.\frac{\partial K_m(kr)}{\partial(kr)}\right|_{r=r_0}$$

The charge per unit length of the perturbed jet is given by

$$Q_p = \frac{1}{\lambda}\int_0^{2\pi}\int_0^{\lambda} \sigma_s \, dS \quad [18]$$

where the differential area dS in cylindrical coordinates is expressed as

$$dS = r_0 \, d\theta \, dz \quad [19]$$

By using [17], [18] and [19] for calculating Q_p correct to second-order, we have

$$Q_p = \frac{2\pi\varepsilon_0 V_0}{\ln 4h/a}\left[1 - \frac{1}{4}\frac{c^2}{a^2} - \frac{1}{4}\frac{c^2 k}{a}\frac{K'_m(ka)}{K_m(ka)}\right] \quad [20]$$

The potential energy per unit length of the jet due to electrification is given as

$$P_p = \frac{1}{2}Q_p V_0 = \frac{\pi\varepsilon_0 V_0^2}{\ln 4h/a}\left[1 - \frac{1}{4}\frac{c^2}{a^2} - \frac{1}{4}\frac{c^2 k}{a}\frac{K'_m(ka)}{K_m(ka)}\right] \quad [21]$$

The charge and the potential energy per unit length of the unperturbed jet are, respectively

$$Q_0 = \frac{2\pi\varepsilon_0 V_0}{\ln 4h/a} \quad [22]$$

$$P_0 = \frac{1}{2}Q_0 V_0 = \frac{\pi\varepsilon_0 V_0^2}{\ln 4h/a} \quad [23]$$

which follow from [20] and [21], respectively, with the perturbation terms set to zero.

The change in the electrostatic potential energy of the charged liquid jet can be calculated with the use of [21] and [23]

$$\tilde{P}_E = P_p - P_0 = -\frac{\pi}{4}\frac{\varepsilon_0 V_0^2}{a^2 \ln 4h/a}\left[1 + ka\frac{K'_m(ka)}{K_m(ka)}\right]c^2 \quad [24]$$

According to Landau and Lifshitz (1960), only the energy of the conducting liquid jet, and not that of the whole system, appears in $\tilde{P}_E$. So $\tilde{P}_E$ pertains to a system which is not energetically closed. For a system whose electric potential is kept constant, the change in electric potential energy is shown to be $P_E = -\tilde{P}_E$.

Generally, we have

$$P_E = \frac{\pi}{4}\frac{\varepsilon_0 V_0^2}{a^2 \ln 4h/a}\left[1 + ka\frac{K'_m(ka)}{K_m(ka)}\right](1 + \delta_m)c^2 \quad [25]$$

The change in the potential energy due to surface tension, P_σ, and the kinetic energy, K, have already been given by Chandrasekhar (1981). They are, per unit length

$$P_\sigma = -\frac{\pi}{4}\frac{\sigma}{a}(1 - m^2 - k^2a^2)(1 + \delta_m)c^2 \quad [26]$$

$$K = \frac{\pi}{4}\frac{\rho a^2}{ka}\frac{I_m(ka)}{I'_m(ka)}(1 + \delta_m)\dot{c}^2 \quad [27]$$

Here

$$I'_m(ka) = \left.\frac{\partial I_{\mathrm{m}}(kr)}{\partial(kr)}\right|_{r=a}$$

σ is surface tension and ρ is liquid density.

Since the Lagrangian L is given by

$$L = K - P_\sigma - P_{\mathrm{E}} \qquad [28]$$

the expression for L is obtained by substituting [25], [26] and [27] into [28].

By substituting [28] into the Lagrange equation of motion for the generalized coordinate c

$$\frac{\mathrm{d}}{\mathrm{d}t}\left(\frac{\partial L}{\partial \dot{c}}\right) - \frac{\partial L}{\partial c} = 0 \qquad [29]$$

we obtain the following differential equation

$$\ddot{c} - \frac{\sigma}{\rho a^3}\frac{kaI'_{\mathrm{m}}(ka)}{I_{\mathrm{m}}(ka)}(1 - m^2 - k^2a^2)c + \frac{\varepsilon_0 V_0^2}{\rho a^4 \ln 4h/a}\frac{kaI'_{\mathrm{m}}(ka)}{I_{\mathrm{m}}(ka)}\left[1 + ka\frac{K'_{\mathrm{m}}(ka)}{K_{\mathrm{m}}(ka)}\right]c = 0 \qquad [30]$$

With the displacement of the surface $c \propto \mathrm{e}^{\omega t}$ the above differential equation reduces to the dispersion equation

$$\omega^2 = \frac{\sigma}{\rho a^3}\frac{kaI'_{\mathrm{m}}(ka)}{I_{\mathrm{m}}(ka)}(1 - m^2 - k^2a^2) - \frac{\varepsilon_0 V_0^2}{\rho a^4 \ln 4h/a}\frac{kaI'_{\mathrm{m}}(ka)}{I_{\mathrm{m}}(ka)}\left[1 + ka\frac{K'_{\mathrm{m}}(ka)}{K_{\mathrm{m}}(ka)}\right] \qquad [31]$$

For the axisymmetric (varicose) mode $m = 0$, by taking into account the fact that

$$I'_0(ka) = I_1(ka)$$
$$K'_0(ka) = -K_1(ka)$$

equation [31] becomes

$$\omega^2 = \frac{\sigma}{\rho a^3}\frac{kaI_1(ka)}{I_0(ka)}(1 - k^2a^2) - \frac{\varepsilon_0 V_0^2}{\rho a^4 \ln 4h/a}\frac{kaI_1(ka)}{I_0(ka)}\left[1 - ka\frac{K_1(ka)}{K_0(ka)}\right] \qquad [32]$$

For the non-axisymmetric (kink) mode $m = 1$, with the use of

$$ka\frac{I'_{\mathrm{m}}(ka)}{I_{\mathrm{m}}(ka)} = ka\frac{I_{\mathrm{m}-1}(ka)}{I_{\mathrm{m}}(ka)} - m$$

$$ka\frac{K'_{\mathrm{m}}(ka)}{K_{\mathrm{m}}(ka)} = -ka\frac{K_{\mathrm{m}-1}(ka)}{K_{\mathrm{m}}(ka)} - m$$

the dispersion relationship yields

$$\omega^2 = -\frac{\sigma}{\rho a^3}k^2a^2\left[ka\frac{I_0(ka)}{I_1(ka)} - 1\right] + \frac{\varepsilon_0 V_0^2}{\rho a^4 \ln 4h/a}\left[ka\frac{I_0(ka)}{I_1(ka)} - 1\right]ka\frac{K_0(ka)}{K_1(ka)} \qquad [33]$$

3. RESULTS AND DISCUSSIONS

Dispersion equation [31] gives the relation between the growth rate ω, the wavelength of the disturbance λ, the applied electric potential V_0, with considering the geometry of the system for liquid spraying and physical properties of the fluid for arbitrary deformations of the charged liquid jet. Since it is assumed that the liquid jet is initially subjected to arbitrary disturbances involving all possible wavelengths, the critical breakup wavelength λ_{cr} corresponds to the maximum value of growth rate ω_{cr}.

If ω^2 is less than zero, the real part of the growth rate ω is zero and the value of ω is imaginary. Since the surface wave amplitude c is proportional to $e^{\omega t}$, negative ω^2 represents oscillatory motion, and the initial disturbance does not grow. Thus the liquid jet becomes stable. If ω^2 is greater than zero, the quantity ω has a positive real value. Positive values of ω correspond to an unlimited growth of the disturbance. The exponential growth of wave amplitude with time leads to instability of the jet surface and breakup of the jet into droplets.

Numerical calculation of the growth rate was carried out for the axisymmetric (varicose) mode $m = 0$ and non-axisymmetric (kink) mode $m = 1$, using [32] and [33], respectively. Here we make use of dimensionless quantities $\omega^{*2} = \omega^2/\sigma/\rho a^3$ and $\lambda^* = \lambda/2\pi a$. The quantities used in the calculations are: water density $\rho = 999$ kg/m^3, surface tension of water in the air $\sigma = 0.0728$ N/m and liquid jet radius $a = 0.1$ mm.

We have also calculated the growth rate for non-axisymmetric modes $m = 2$ and $m = 3$, using [31]. The results of calculation showed that $\omega^{*2}_{m=1} > \omega^{*2}_{m=2} > \omega^{*2}_{m=3}$. The fact that the kink mode $m = 1$ has the highest growth rate of all other non-axisymmetric modes means that the kink mode $m = 1$ is prevalent over other non-axisymmetric modes. This fact is also supported by our experimental observations. Hence we represent here the numerical results for only the kink mode $m = 1$.

In the case of uncharged liquid jet (applied voltage $V_0 = 0$), the expressions for growth rate of varicose and kink modes could be obtained from [32] and [33], respectively, by setting the second term of the right-hand side, which contains the quantity V_0, to zero.

For the varicose mode, the growth rate reads

$$\omega^2 = \frac{\sigma}{\rho a^3}\frac{kaI_1(ka)}{I_0(ka)}(1 - k^2a^2) \qquad [34]$$

This is the well-known result obtained by Rayleigh. It is clear that the liquid jet is unstable when $ka > 1$ or $\lambda > 2\pi a$, i.e. when the wavelength is greater than the periphery of the liquid jet. The critical maximum growth rate occurs at $\lambda_{cr}/2\pi a = 1.44$, or $\lambda_{cr} = 9.05a$.

For the kink mode, we have

$$\omega^2 = -\frac{\sigma}{\rho a^3}k^2a^2\left[ka\frac{I_0(ka)}{I_1(ka)} - 1\right] \qquad [35]$$

In this case, ω^2 is negative for any ka. Thus, the kink mode does not take place for the uncharged liquid jet. This statement has also been made by Rayleigh. It is worth to note here that in the present analysis, the velocity of the liquid jet is considered to be small and the interaction of the jet with surrounding medium is negligible.

The growth rates for the case $V_0 = 0$ are shown on figure 3a.

The effects of the electric field strength are investigated through two parameters: applied voltage and needle-plate distance. The increase in electric field strength means the increase in applied voltage and/or shortening of the needle-plate distance. It is clear that with increasing electrical charge the critical wavelength λ^*_{cr} is decreased. For example, for the needle-plate distance $h = 20$ cm, λ^*_{cr} of the varicose mode shifts from 1.20 as $V_0 = 2$ kV (see figure 3a) to 0.63 as $V_0 = 4$ kV and gets 0.31 as $V_0 = 6$ kV (see figure 3b). This tendency continues with further increasing in V_0 and is similar for the kink mode. The decrease in the critical wavelength evidently leads to the disintegration of the liquid jet into the droplets with smaller size.

As indicated on figure 3, in the case of low applied voltage V_0 the critical growth rate ω^{*2} for the varicose mode is larger than that of the kink mode, while the corresponding critical wavelength λ^*_{cr} for the varicose mode is smaller than that of the kink mode (see figure 3a). Therefore the varicose mode has a dominant effect on the instability of liquid jet at the short wavelength at low voltage. However with the further increase in the applied voltage V_0 the critical growth rate of the kink mode increases rapidly and eventually approaches the critical growth rate of the varicose mode at the same critical wavelength at about 10 kV (see figure 3b). Hence the link mode is more pronounced the higher the electrical charge. However, these calculated results of the present theoretical analysis leave the question whether the varicose or the kink mode has a

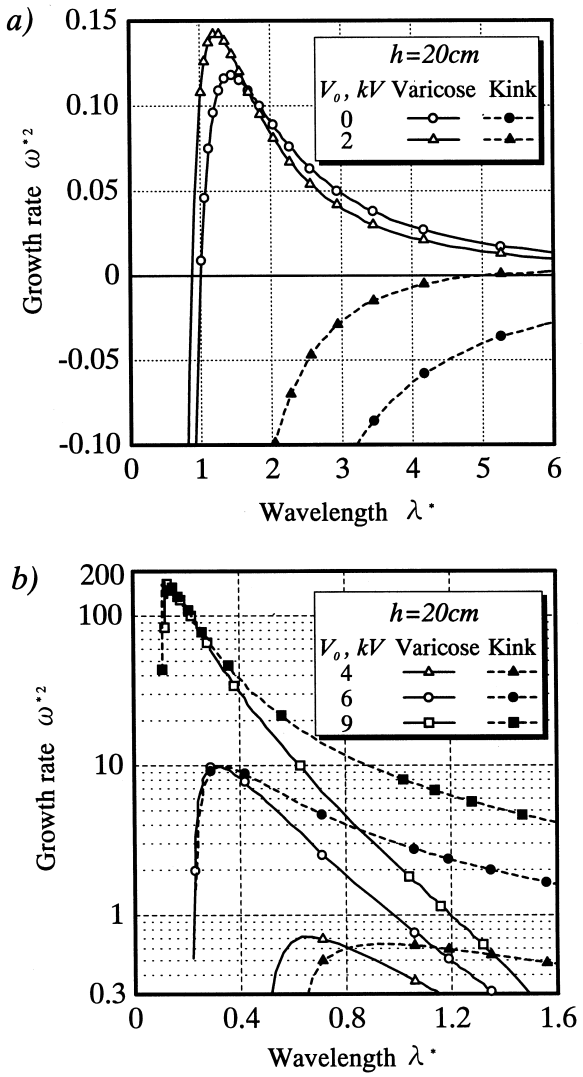

Figure 3. Growth rate variation with applied voltages at needle-plate space $h = 20$ cm.

dominant effect in the range of short wavelength at high applied voltage unanswered since the critical growth rates and critical wavelengths of both the varicose and kink modes are of the same magnitude. Besides, in the case of high applied voltage the instability of the liquid jet at long wavelength can not be predicted by this theory since the critical growth rate appears in the short wavelength ranges.

We can see from the figure 3 that as the voltage is increased, the critical growth rate is increased too. The dimensionless critical growth rates ω^{*2} of the varicose mode are 0.142, 0.714 and 9.928, and those of the kink mode are 0.003, 0.564 and 9.849 for applied voltages 2, 4 and 6 kV, respectively. In jet breakup the larger the critical growth rate, the shorter the length of the liquid jet prior to breakup.

As the needle-plate distance h is shortened, the behavior of the instability modes, and thus the phenomenon of breakup of the liquid jet has the same tendency such as when the electric potential is increased. The growth rate variation with needle-plate distance is given in figure 4.

Thus, the analytical results presented here exhibit that the instability modes and disintegration of the electrically charged liquid jet strongly depend upon the electrical field strength.

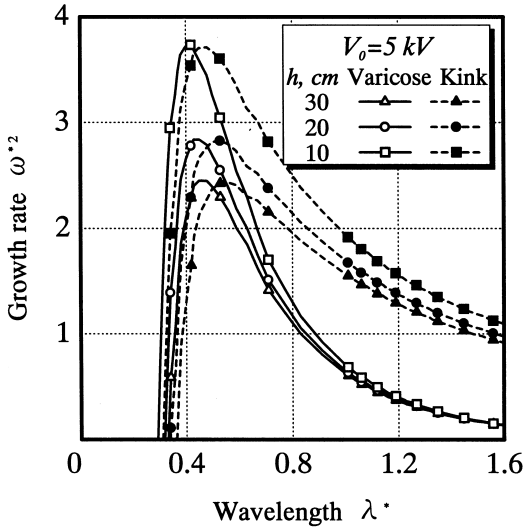

Figure 4. Growth rate variation with needle-plate spaces at applied voltage $V_0 = 5$ kV.

4. COMPARISON WITH EXPERIMENTAL RESULTS

The needle-plate apparatus for liquid spraying (see figure 2) is used in the present experiments. A stainless steel needle is of 0.2 mm and 0.4 mm in inner and outer diameters respectively. The needle is placed at 10, 20 and 30 cm above an electrically grounded funnel. A positive DC high voltage up to 40 kV is applied to the needle. Distilled water is fed to the needle by a microtube pump at the mass flow rates $\dot{m}$ ranged from 1 to 3 g/min. The behavior of the liquid jet deformation and droplet formation process are recorded by using a high speed video camera at 500 frames/s.

Since a high electric potential is applied to the small stainless steel needle and the plate is electrically grounded, the electric field is extremely high in the region around the needle tip with very small radius of curvature compared to the region near the edge of the grounded plate, whose diameter is 45 cm and much larger than the needle. The jet instability and its disintegration process is sensitive to the electric field strength. Thus, the region near the needle tip with high electric field strength and charge density is thought to have a deciding effect on the liquid jet deformation and disintegration.

The photographs of the liquid jet deformation obtained at $h = 20$ cm and $\dot{m} = 3.07$ g/min are shown in figure 5. At the applied voltages below 10 kV only the varicose mode takes place, which is consistent with the analytical results. At the potential larger than 10 kV the kink mode appears but only slightly. As the voltage increases furthermore, a stronger waving motion of the liquid jet occurs. We can see in these pictures the coexistence of the varicose and kink modes at high voltage. However, the kink mode of the liquid jet instability always takes place at long wavelength, which is in contrast with the theoretical results. The reason is possibly that this theoretical analysis is based on the assumption that the deformation of liquid jet from its equilibrium shape is very small relative to the jet radius. Therefore, it might not accurately describe the development of the waves on the surface of the liquid jet when their amplitude becomes large.

The difference between the experimental and theoretical results can be seen in figure 6. In this graph, the measured wavelengths of liquid jet prior to breakup and the calculated critical wavelengths are plotted. For the varicose mode, the theoretical critical wavelength decreases much faster than the experimental one as the applied voltage increases. The kink mode of liquid jet deformation is observed to occur at higher voltage and with wavelength much larger than that obtained from the theoretical analysis. Here, the fact that the velocity of the liquid jet injected from the needle and the influence of the surrounding air on the development of the wave on the liquid jet surface are neglected in the present analysis may lead to the aforementioned disagreements between the theoretical and experimental results. Moreover, the present theoretical model is based on the assumption of inviscid fluids. So it can not account for the effect of shear stress

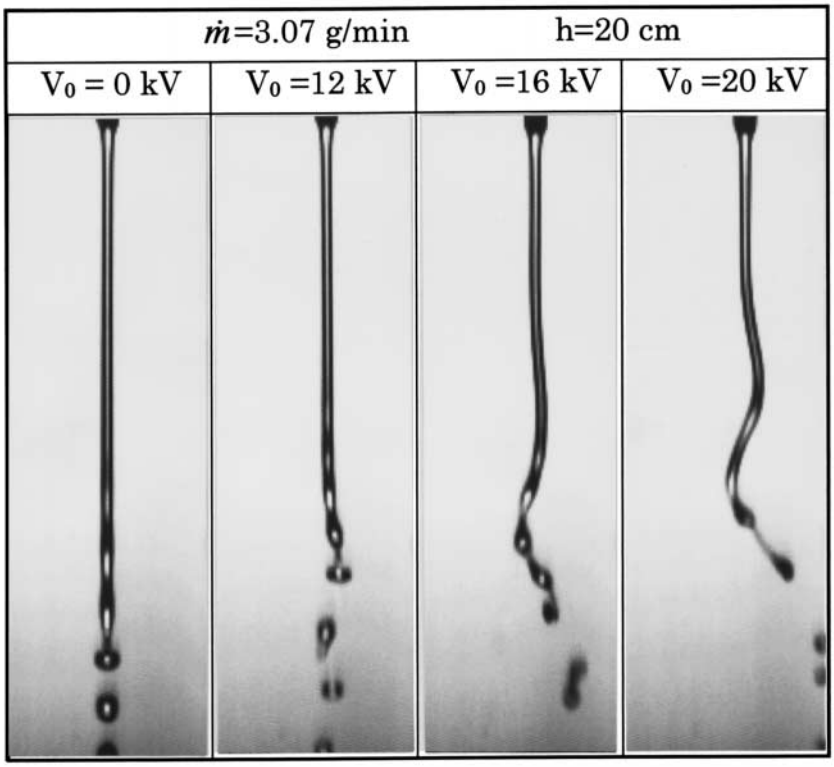

Figure 5. Photographs of the liquid jet injected into still air for various applied voltages at mass flow rate $\dot{m} = 3.07$ g/min.

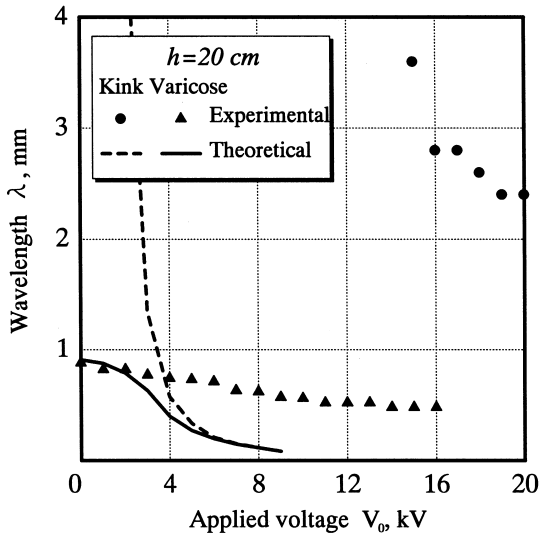

Figure 6. Experimental and theoretical wavelengths variation with applied voltages for needle-plate space $h = 20$ cm. The experimental data are obtained at mass flow rate $\dot{m} = 3.07$ g/min.

acting on the liquid jet surface, which may play an important role in the development of surface disturbances.

5. CONCLUDING REMARKS

Some previous theories on electrohydrodynamic jet atomization are limited to axisymmetric deformation of the jet surface. They are not capable of predicting commonly observed sinuous

deformation, or snake-shape of the jet. The present study derived a dispersion equation that accounts for the growth of the axisymmetric, as well as the non-axisymmetric disturbances with taking into account the electric field configuration of the needle-plate system for liquid spraying. The calculation of the growth rate of disturbances on the surface of the electrically charged liquid jet from the available dispersion equation, which is derived from the Lagrange equation of motion, reveals the following facts.

1. For low electric field strength, the axisymmetric mode has a higher growth rate than that of the non-axisymmetric one at all wavelength ranges. With increasing in electric field strength, the growth rate of non-axisymmetric mode grows more rapidly and eventually approaches that of axisymmetric mode. As a result, the present theory well predicts the varicose deformation of the charged liquid jet at low electric field strength and its possible snake-shape deformation at high electric field strength.
2. With increasing applied voltage and/or shortening needle-plate distance, i.e. increasing electric field strength, the critical wavelength is decreased and the critical growth rate is increased. These mean that the droplet size is reduced and the liquid jet length is shortened, which are qualitatively consistent with the experimental results.

However, the calculated critical wavelengths appear to be small at high electric field strength, which are in contrast with those obtained experimentally, in particular, for the kink mode. The kink mode in fact takes place only at long wavelength ranges. This phenomenon can not be predicted by the present theoretical analysis. It is thought that the velocity of the liquid jet and the influence of the surrounding air, as well as the liquid viscosity are necessary to be taken into account for the instability analysis of the liquid jet.

Acknowledgements—The authors would like to acknowledge Associate Professor K. Bando and Research Associate A. Sakurai of Kansai University for many valuable comments and discussions. The authors are also indebted to graduate students N. Takebe and T. Hosokawa for obtaining most of the experimental data.

REFERENCES

Bailey, A. G. (1974) Electrostatic atomization of liquids. *Sci. Prog. Oxf.* **61,** 555–581.

Bailey, A. G. (1986) The theory and practice of electrostatic spraying. *Atomisation Spray Technology* **2,** 95–134.

Chandrasekhar, S. (1981) *Hydrodynamic and Hydromagnetic Stability*. Dover, New York.

Cloupeau, M. and Prunet-Foch, B. (1990) Electrostatic spraying of liquids: main functioning modes. *J. Electrostatics* **25,** 165–184.

Cloupeau, M. and Prunet-Foch, B. (1994) Electrohydrodynamic spraying functioning modes: a critical review. *J. Aerosol Sci.* **25,** 1021–1036.

Huebner, A. L. and Chu, H. N. (1971) Instability and breakup of charged liquid jets. *J. Fluid Mech.* **4,** 361–372.

Jones, A. R. and Thong, K. C. (1971) The production of charged monodisperse fuel droplets by electrical dispersion. *J. Phys. D: Appl. Phys.* **4,** 1159–1165.

Landau, L. D. and Lifshitz, E. M. (1960) *Electrodynamics of Continuous Media*. Pergamon, New York.

Schneider, J. M., Lindblad, N. R., Hendricks, C. D. and Crowley, J. M. (1967) Stability of an electrified liquid jet. *J. Appl. Phys* **38,** 2599–2605.

Lord, Rayleigh J. W. S. (1882) On the equilibrium of liquid conducting masses charged with electricity. *Phil. Mag.* **14,** 184–186.

Lord, Rayleigh J. W. S. (1945) *The Theory of Sound*, Vol. 2. Dover, New York.